PERGAMON

Available at
www.ElsevierComputerScience.com
POWERED BY SCIENCE DIRECT®

Pattern Recognition 38 (2005) 133–142

PATTERN RECOGNITION
THE JOURNAL OF THE PATTERN RECOGNITION SOCIETY

www.elsevier.com/locate/patcog

ECG to identify individuals

Steven A. Israel[a,*], John M. Irvine[b], Andrew Cheng[b], Mark D. Wiederhold[c], Brenda K. Wiederhold[d]

[a]*SAIC, 4001 Fairfax Drive, Suite 450, Arlington, VA 22203, USA*
[b]*SAIC, 20 Burlington Mall Road, Burlington, MA 01803, USA*
[c]*SAIC, 10260 Campus Point Drive, San Diego, CA 92121, USA*
[d]*Virtual Reality Medical Center, 6160 Cornerstone Drive, San Diego, CA 92121, USA*

Received 22 October 2003; accepted 21 May 2004

Abstract

The electrocardiogram (ECG also called EKG) trace expresses cardiac features that are unique to an individual. The ECG processing followed a logical series of experiments with quantifiable metrics. Data filters were designed based upon the observed noise sources. Fiducial points were identified on the filtered data and extracted digitally for each heartbeat. From the fiducial points, stable features were computed that characterize the uniqueness of an individual. The tests show that the extracted features are independent of sensor location, invariant to the individual's state of anxiety, and unique to an individual.

Keywords: Electrocardiogram (ECG); Biometrics; Human identification; Classification; Discriminant analysis; Stress invariance

1. Introduction

Electrocardiogram (ECG) data are traditionally acquired for clinical diagnosis of cardiac function. Dubin [1] describes the link between cardiac function and the expression of the ECG trace. In addition, he offers a set of rules for ECG interpretation. However, Dubin's work uses analog methods for applying these rules. With the advances in computational power and medical instrumentation, hardware/software systems have been developed for assisted ECG trace interpretation (e.g. Siemens Medical <www.smed.com> and Thought Technologies <www.thoughttechnology.com>).

The ECG trace contains a wealth of information. Researchers have been using ECG data as a diagnostic tool since the early 20th century. Only in the last 20 years, however, have researchers been able to apply digital analysis to the data [2]. The most common digital application is heartrate variability (HRV) [3]. Researchers have applied numerical methods to more complex diagnostic interpretation tasks such as demixing mother–fetal signal [4], identifying atrial and ventrical fibrillation [5,6], myocardial infarction [7] and recently to characterize the uniqueness of the ECG to an individual [8–11]. Except for the HRV studies, each researcher has developed ad hoc features.

In this paper, we propose a more extensive set of ECG descriptors that more completely characterize the trace of a heartbeat. The proposed ECG descriptors contain information about the physiology of an individual's heart, rather than some visual expression of traits [9]. As a biometric, heartbeat data are difficult to disguise, reducing the likelihood

* Corresponding author. Tel.: +1-703-248-7706; fax: +1-703-522-6006.
E-mail address: steven.a.israel@saic.com (S.A. Israel).

0031-3203/$30.00
doi:10.1016/j.patcog.2004.05.014

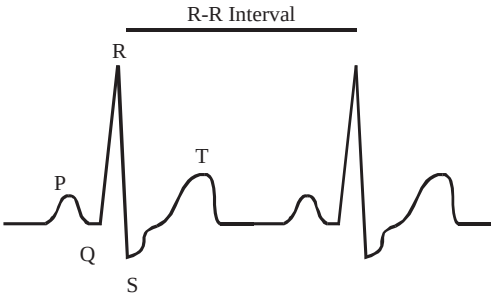

Fig. 1. Ideal ECG signal: This figure depicts two idealized heartbeats. The R–R interval indicates the duration of a heartbeat. The major ECG complexes comprising one heartbeat are indicated by P, QRS, and T.

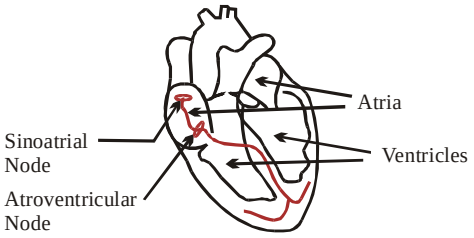

Fig. 2. The heart and its pacemakers: The sinoatrial node is the heart's primary pacemaker. The atrioventricular node forces the time lag between the atrial and the ventricular contraction.

of successfully applying falsified credentials into an authentication system.

2. Mechanics of the ECG

The ECG signal measures the change in electrical potential over time. The trace of each heartbeat consists of three complexes: P, R, and T. These complexes are defined by the fiducial that is the peak of each complex (Fig. 1). The labels in Fig. 1 document the commonly used medical science ECG fiducials.

A heartbeat is the physical contraction of the heart muscle caused by chemical/potential differences in the component cells called myocytes. The myocytes have negatively charged interiors. The heartbeat begins with the firing of the Sinoatrial (SA) node. The SA node (Fig. 2) is the heart's dominant pacemaker. The electrical signal radiates outward causing the myocytes to depolarize and compress rapidly by a movement of sodium (NA^+) ions. This is expressed as P wave of the ECG trace. The depolarization rate slows dramatically when the signal hits the atrio-ventricular (AV) node, where the chemical signal changes to relatively slow moving calcium (CA^+) ions. The change in contraction is expressed as the gap between the P and the R complexes. Once past the AV node, the signal passes through to the cells lining the ventricles. The ventricles contract rapidly, which produces the R complex. Repolarization does not exactly mirror polarization due to the chemical agents and the lag between the end of the electrical impulse and physical displacement [1].

The heartrate is controlled by the autonomic nervous system (ANS). ANS is composed of the sympathetic and parasympathetic system. Each of the two systems has independent ganglia and secretes neurotransmitters. The sympathetic system stimulates the cardiovascular system by increasing the rate of SA node firing, increasing the mycocyte cell conductivity, and increasing the force of contraction. The results of the sympathetic secretion of neurotransmitters are: 1. the reduction of the interbeat interval due to the increased SA firing rate, and 2. the reduction in the width of the P and T complexes due to increase conductivity. The parasympathetic system has the opposite effect.

The ECG is measured with respect to an arbitrary baseline. The magnitude of the electrical potential varies with the placement of electrodes relative to the heart. Diagnosticians have exploited the change in information with sensor placement to improve their understanding of cardiac performance.

3. ECG data

For this experiment, data were collected from males and females between the ages of 22 and 48. Twenty-nine individuals were tested with 12 repeat sessions for a total of 41 sessions within the data set. Each individual session contained a set of seven two-minute tasks. The tasks were designed to stimulate different states of anxiety. Unlike conventional ECG data, the hardware for this series of experiments collected ECG data at high temporal resolution, 1000 Hz. Fig. 3 is a waterfall diagram of ECG traces that shows the differences among subjects and tasks. Each block of seven heartbeats is the average of the heartbeats for that individual performing each of the seven tasks. The subject-to-subject differences are visually greater than task differences, a surrogate for level of stress.

The remainder of this paper is arranged by the ECG processing stage. The first half of the paper discusses the unique data processing stages required to identify individuals. The latter half of the paper shows the results for the sensor placement, state of anxiety, and identifying individuals tests. The paper concludes with a discussion of how the results support our conclusion that ECG data is unique to an individual and that the features extracted are a viable biometric.

4. ECG processing

To realize the ideal data structure (Fig. 1), the raw ECG data must be processed to remove the non-signal artifacts. The first step is to identify the noise sources. Based upon the structure of these noise sources, a filter is designed and

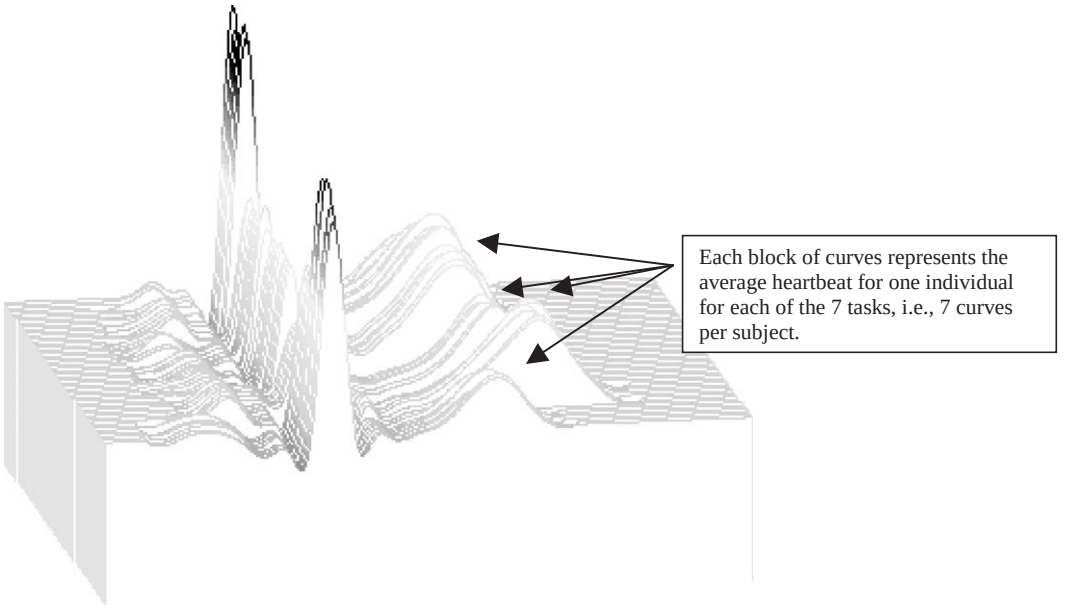

Fig. 3. Heartbeats averaged by subject and task.

applied to the raw data. The filtered data is used to locate fiducials and to perform feature extraction. To best convey the processing hierarchy, all of the figures generated in this paper originate from a common data series.

4.1. Noise sources

Fig. 4a and b show the data sample of the high resolution ECG data. The figures show that the raw data contain both high and low frequency noise components. These noise components alter the expression of the ECG trace from its ideal structure (Fig. 1). The low frequency noise is expressed as the slope of the overall signal across multiple heartbeat traces in Fig. 4a. The low frequency noise is generally associated with changes in baseline electrical potential of the device and is slowly varying. Over the 20 s segment, the potential change of the ECG baseline inscribes approximately 1 1/2 wave periods. The high frequency noise is expressed as the intrabeat noise shown in Fig. 4b. The high frequency noise is associated with electric/magnetic field of building power (electrical noise) and the digitization of the analog potential signal (A/D noise).

Plotting the Fourier power spectra illustrates the various elements of the ECG signal. In this case, we plotted the 20,000 raw samples over 16384 (2^{14}) frequencies. In Fig. 5a, three fundamental frequencies are readily identified: the 60 Hz electrical noise due to the US power line, the 1.10 Hz heartbeat information (approximately 22 heartbeats in 20 s), and the 0.06 Hz change in baseline electrical potential (approximately 1 1/2 wave periods in 20 s). The remainder of the frequency power spectra is a combination of other noise sources and subject information. The goal of filtering is to remove the 0.06 and 60 Hz noise while retaining the individual heartbeat information between 1.10 and 40 Hz. The filter curve represents the frequency bandpass acceptance region.

Examination of multiple filtering techniques showed that local averaging, spectral differencing, and Fourier bandpass filtering held promise. The filter's design constraints were:

1. Maintain as much of the subject dependent information (signal) as possible.
2. Reduce the data to best resemble the idealized heartbeat (Fig. 1).
3. Design a stable filter across all subjects.

After applying each filtering technique to the data, the best method was observed to be band pass filtering. We reviewed the required bandpass limits and developed a filter that takes advantages of the limitations of filtering cited above. By observing Fig. 5a, a considerable gap exists between the subject information (43 Hz) and the 60 Hz noise. The gap at the high frequency will change with heartrate and individual. The same factors occur at the low frequency end at approximately 2 Hz.

Our filtering solution merges heuristic and quantitative information and mathematics, using a frequency bandpass filter between 2 and 40 Hz. However, the filter is written using the equivalent of a lower order polynomial. This filter allows 'advantageous' bleeding of information into the processed data stream (Fig. 6 b). The lower order polynomial filter is stable at the frequency limits, which is important at the low frequency edge. The resulting post filtering power spectrum is shown in Fig. 5b. After filtering, the heartbeats

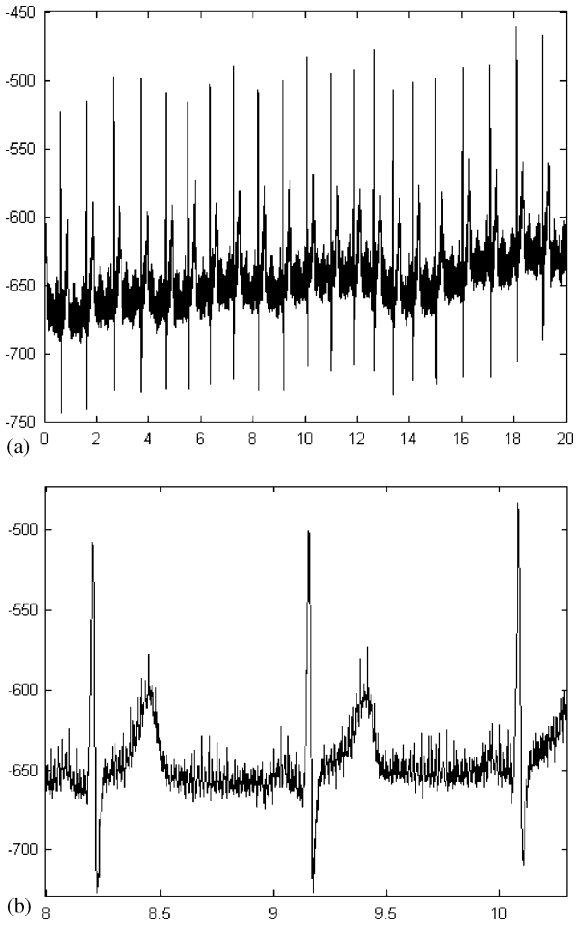

Fig. 4. Raw ECG data 1000 Hz: (a) 20 s; (b) 2 s; The *Y* axis is electrical potential and the *X* axis is time in seconds.

for each data segment were aligned by their R peaks in a waterfall diagram (Fig. 3).

4.2. Fiducial points

Once the non-signal components were removed from the ECG data stream, the ECG trace fiducial positions were located. The standard medical fiducial labels do not fully characterize the entire heartbeat trace. From pattern recognition science, additional feature attributes are rarely completely correlated or independent. However, additional subject attributes generally improve the scalability to larger populations [13] at the cost of reducing the tolerance intra-subject variability.

For human identification, attributes were extracted from the P, R, and T complexes (Fig. 7). Four additional fiducial points were identified. The locations of the four new fiducial positions, noted by an apostrophe (‘), are at the basal positions of the P and T complexes (Fig. 7). Collectively, the fiducials exploit the unique physiology of an individual. Physically, the L’ and P’ fiducials indicate the start and end of the atrial depolarization. The corresponding S’ and T’ positions indicate the start and end of ventricular repolarization.

The fiducial points were extracted in the time domain in two stages. The peaks were established by finding the local maximum in a region surrounding each of the P, R, and T complexes. The base positions were determined by tracking downhill and finding the location of the minimum radius of curvature (Fig. 8). The minimum radius of curvature proved more robust to local noise than the more obvious derivative measures. By fixing the time difference between X and Y and X and Z, the minimum radius of curvature is found by maximizing the value of δ using the vector cross product between the two directed line segments.

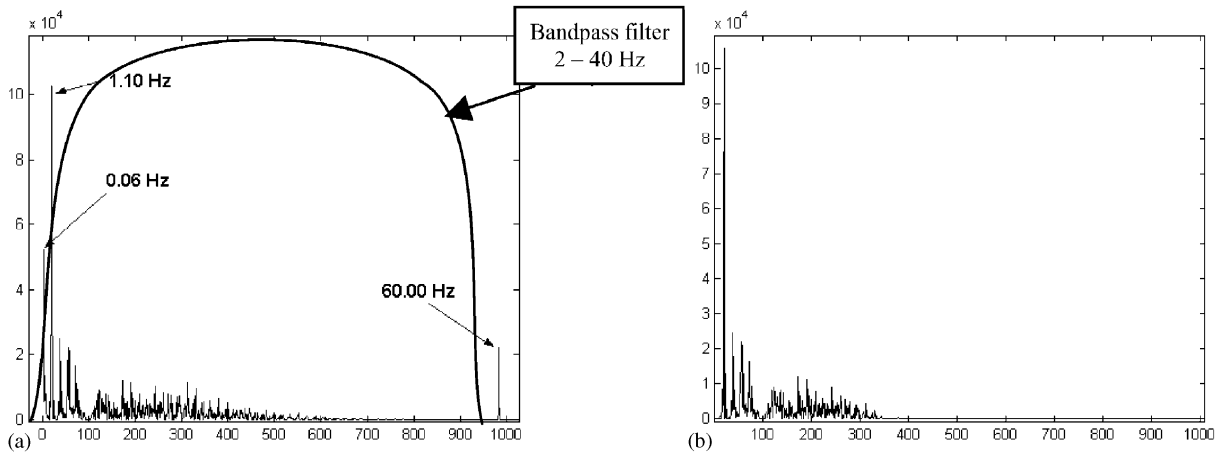

Fig. 5. Power spectra of frequency filtering: (a) bandpass filter of raw data; (b) frequency response of filtered data. (a) shows the noise source spikes at 0.06 and 60 Hz and the information spikes between 1.10 and 35 Hz. (b) shows the filtered data with the noise spikes removed and the subject specific information sources retained.

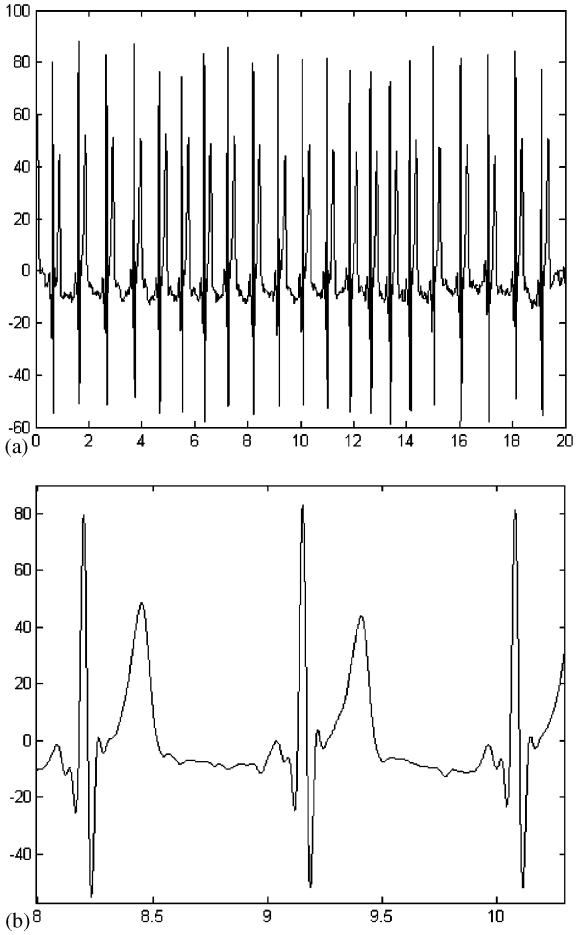

Fig. 6. Bandpass filtered ECG trace: (a) entire range of data; (b) segment of data. The results of applying the filter (Fig. 5) to the raw (Fig. 4) data are shown to closely replicate the idealized (Fig. 1) ECG without noise.

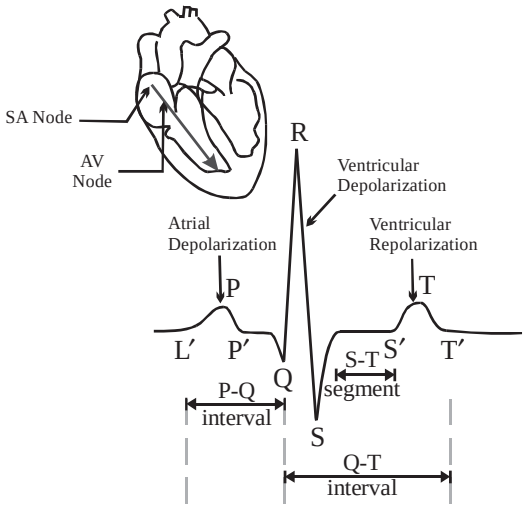

Fig. 7. ECG trace based upon cardiac physiology [12]. L' and P' indicate the start and end of atrial depolarization, the R complex indicates ventricular depolarization, and the T complex indicates the ventricular repolarization.

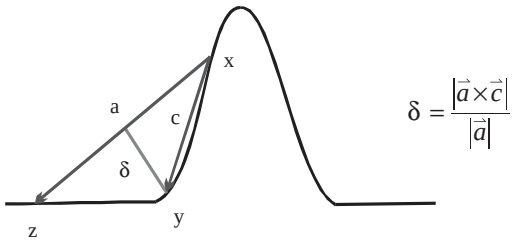

Fig. 8. Radius of curvature: By fixing the time difference between *X* and *Y* and *X* and *Z*, the radius of curvature is computed as the vector cross product between the two directed line segments.

4.3. Features

The expression of the ECG trace is a function of sensor placement for electrical potential magnitude only. The sensor position does not affect the observed timing of the individual P, R, and T complexes. Therefore, the temporal distances among the fiducial points are independent of the sensor placement (data analysis for this is shown in Section 5.1). Since the heartbeat's R position was used for aligning the waterfall diagram, the distances were computed from the other fiducial points to the R position (Fig. 9). These computational distances are unsigned. An additional process is required to account for changes in these individual distances with changes heartrate.

The distances between the fiducial points and the R position vary with heartrate. If a linear relationship exists between heartrate and those distances, normalization would be computed as the extracted distance divided by the L'T' distance. This approach effectively scales the heartbeat to a unit length. The normalized features represent the relative positions of the fiducials within a heartbeat. The linear normalization has a heuristic rather than a physiological basis. The distance that an electrical impulse travels along the atrial axis is fixed, so that changes in heartrate are not evenly distributed across the P, R, and T complexes.

To better understand how normalization should occur, a review of the underlying physiology is required. The interbeat interval (T' of the previous heartbeat to L' of the current heartbeat) is a transition stage that is independent of the electrical timing mechanism. The R complex is a trigger for the ventricular contraction. As an electrical trigger, it is a function of distance and not heartrate. As such, it remains

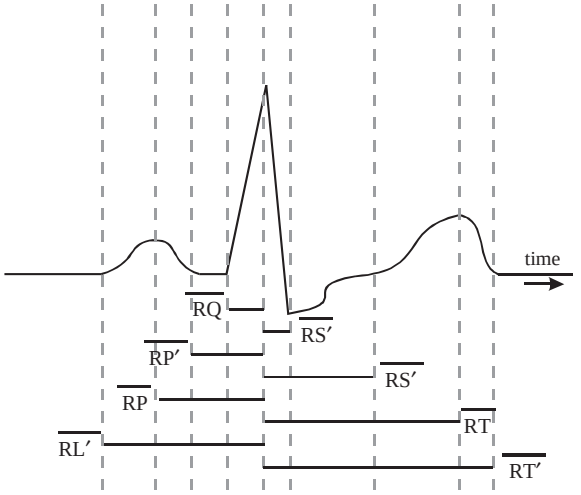

Fig. 9. Extracted distance among the ECG fiducials.

Extracted Attributes		
1. RQ	**6.** RT	**11.** ST
2. RS	**7.** RS'	**12.** PQ
3. RP	**8.** RT'	**13.** PT
4. RL	**9.** P width	**14.** LQ
5. RP'	**10.** T width	**15.** ST'

Fig. 10. Extracted attributes. The feature list labels are the normalized distance between the two fiducials. For example RP' is the unsigned distance between the end of the P-wave and the R peak.

fairly constant with changes in heartrate. So, the principal mechanisms of heartrate changes are caused by atrial depolarization (P complex) and ventricular repolarization (T complex). These two events are the dominant causes to the changes in pressure within the heart and ventricular volume. The values for P and T complex distances were normalized by dividing by the L'T' distance. Raw RQ and RS distances are used as features. In total 15 features were extracted from each heartbeat (Fig. 10).

Within each subject session, each two-minute task was divided into six twenty-second segments. During feature extraction either all features were identified for an individual heartbeat, or the heartbeat was removed from further analysis. Outliers were removed iteratively so that 70% of the original heartbeats were retained. Low heartbeat count segments were also removed. The segregation of the task data into 20 s segments allowed for independent block training of the discriminant functions.

5. ECG testing

From the original 15 attributes, 12 attributes were commonly selected during the majority of experimental constraints of canonical relationships. A stepwise canonical correlation that used the Wilkes' lambda as a divergence measure provided the feature selection [14]. The feature selection process was performed to ensure stable discrimination.

Classification was performed on heartbeats using standard linear discriminant analysis. A conversion is required to link the performance of the heartbeat classification to human identification. Standard, majority, voting was used to assign individuals to heartbeat data. The conversion was performed using contingency matrix analysis (Fig. 11a).

The contingency matrix, Fig. 11, is a visualization for classification performance [15]. The columns represent the known input data, generally the test examples. The rows indicate how the discriminant function(s) classified the data. The correctly identified samples (heartbeats) lie along the major diagonal. If the maximum number of heartbeats within a row or column occurs along the major diagonal, then the subject is correctly identified; i.e., voting. Errors occurring along the column are errors of omission. For a verification system, these are false negative errors where an authorized user cannot gain access. Errors along the row are errors of commission. Commission errors are false acceptance errors, where an unauthorized user gains accesses the system. The identification error rates cited in this paper are the average of the omission and commission values.

Fig. 11a highlights a number of interpretation issues. First, the contingency matrix is not symmetrical. So, the rate of false acceptance between individuals is not the same. The number of heartbeats acquired is not the same for all individuals. The variable number of examples percolates through the contingency matrix. For Subject B, approximately 30% of the heartbeats have a commission error with Subject J. These heartbeats are over 50% of the total assigned to Subject J. If the two subjects contained the same number of heartbeats, then no confusion or false acceptance of Subject B to Subject J would occur. A normalization procedure, called iterative proportional fitting [16], could be applied if it were assumed that the number of heartbeats from all individuals is the same (Fig. 11b). For these experiments, no assumptions about the relative likelihoods for assigning heartbeats were made.

5.1. ECG features and sensor location

As part of understanding the how well the ECG biometric can be exploited for identifying individuals, this section focuses on the relationship between changes in the ECG lead placement and identification performance. The hypothesis is that the extracted ECG attributes are invariant to placement of the ECG leads. To test this hypothesis,

(a)

computational outputs	known inputs A	B	C	D	E	F	G	H	I	J	K		sum	1-comiss	identified
A	**52**	15			10					1			**78**	**67**	**1**
B	15	**165**											**180**	**92**	**1**
C		**6**	**9**		6								**75**	**92**	**1**
D			1	**125**							9		**135**	**93**	**1**
E	7				**76**								**83**	**92**	**1**
F				5		**77**					6		**88**	**88**	**1**
G							**65**		1		2		**68**	**96**	**1**
H								**154**	12				**166**	**93**	**1**
I								11	**50**				**61**	**82**	**1**
J		85								**76**			**161**	**47**	**0**
K				35		3	2				**49**		**89**	**55**	**1**
											total correct	**958**			**% false pos**
sum	**74**	**265**	**70**	**165**	**92**	**80**	**67**	**165**	**63**	**77**	**66**	total avail	**1184**		**9**
1-omiss	**70**	**62**	**99**	**76**	**83**	**96**	**97**	**93**	**79**	**99**	**74**		% correct	**81**	
identified	**1**	**1**	**1**	**1**	**1**	**1**	**1**	**1**	**1**	**1**	**1**	**% False**	**neg**		
1=correct												**0**			

(b)

computational outputs	known inputs A	B	C	D	E	F	G	H	I	J	K		sum	1-comiss	identified
A	**.72**	.09			.10					.08			**0.99**	**73**	**1**
B	.17	**.83**											**1.00**	**83**	**1**
C		**.**	**98**		.02								**1.00**	**98**	**1**
D			.02	**.80**							.18		**1.00**	**80**	**1**
E	.11				**.89**								**1.00**	**89**	**1**
F				.01		**.93**					.05		**0.99**	**94**	**1**
G							**.96**		.01		.03		**1.00**	**96**	**1**
H								**.89**	.11				**1.00**	**89**	**1**
I								.12	**.88**				**1.00**	**88**	**1**
J		.08								**.92**			**1.00**	**92**	**1**
K				.17		.06	.03				**.73**		**0.99**	**74**	**1**
											total correct	**10**			**% false pos**
sum	**1.00**	**1.00**	**1.00**	**.98**	**1.01**	**.99**	**.99**	**1.01**	**1.00**	**1.00**	**.99**	total avail	**11**		**0**
1-omiss	**72**	**83**	**98**	**82**	**88**	**94**	**97**	**88**	**88**	**92**	**74**		% correct	**87**	
identified	**1**	**1**	**1**	**1**	**1**	**1**	**1**	**1**	**1**	**1**	**1**	**% False**	**neg**		
1=correct												**0**			

Fig. 11. (a) Sample contingency matrix; (b) normalized contingency matrix. These tables show the classification rate for the individual heartbeats. Based on voting, the marginal statistics show the classification of subjects. A '1' in the *identified* row indicates that the correct subject identification.

Assay	Training Data	Heartbeats Classified	Individuals Classified
Locational Invariance	Neck	82%	100%
	Chest	79%	100%

Fig. 12. Classification performance with chest and neck data for training and test. Classification accuracies are an average of omission and commission error.

we collected ECG data at two electrode placements during each session. The sensor placement locations were at the base of the neck and fifth intercostal spacing (chest). We found a strong agreement between neck and chest ECG data (Fig. 12). The performance was determined by training the discriminant functions with the neck data and classifying the chest data. An additional set of discriminant functions was generated by training on the chest data and classifying the neck data. The scores are given for both the heartbeat and subject identification.

5.2. ECG features and state of anxiety

An individual's emotional state is continually changing. These changes occur naturally as a result of body chemistry, level of stress, and even time of day. The changes in emotional state are expressed in the ECG trace as changes in heartrate, noise in trace due to muscle flexor action, and variations in electrical potential gain. The hypothesis is that the normalized features extracted for human identification are invariant to the individual's state of anxiety. To prove this four experiments were performed to test within anxiety and across anxiety states.

1. Discriminant functions trained from low stress conditions could identify the same individuals under low stress conditions.
2. Discriminant functions trained from high stress conditions could identify the same individuals under high stress conditions.
3. Discriminant functions trained from high stress conditions could identify the same individuals under low stress conditions.
4. Discriminant functions trained from low stress conditions could identify the same individuals under high stress conditions.

The seven task protocol was divided into high stress and low stress tasks. The low stress tasks were the subject's baseline state, meditative, and recovery tasks. The high stress tasks were reading aloud, mathematical manipulation, and driving in virtual reality.

Assay	Training Data	Heartbeats Classified	Individuals Classified
Within Anxiety State	Low	83%	97%
	High	78%	97%
Between Anxiety State	Low	66%	98%
	High	63%	98%

Fig. 13. Classification performance for within and between anxiety state, 'Low' indicates low stress tasks and 'High' indicates high stress tasks.

Fig. 13 shows the results for characterizing an individual based upon their level of anxiety. Both within and between anxiety states, nearly all the individuals were correctly classified. The results indicate that the extracted features are invariant to anxiety state.

5.3. ECG feature as a biometric

To use ECG as a biometric, individuals will enroll their information into the security system. After enrollment, the user's ECG will be interrogated by the system. The state of anxiety and the relative orientation of the ECG electrodes with respect to their heart's potential center are unknown. As the number of access controllers and individuals within a facility increases, the number of interrogations grows rapidly. To mitigate data handling issues, the number of descriptors for a given individual must be minimized.

The results show a high degree of agreement of generalization across the tasks, except for the VR driving. During VR driving, many of the subjects' data still contained muscle flexor noise that was not removed with the current filter. We are exploring improvements in the processing techniques to minimize these problems (Fig. 14).

In order to understand the extent that the data were able to generalize, discriminant functions were generated by training on the tasks individually and then block segmentation across tasks. If the features were completely invariant to anxiety state, then an operational enrollment and deployment scheme would be simplified. Fig. 15 shows the results of the identification performance for a many-to-many classification strategy.

6. Discussion

The ECG data can be easily manipulated using traditional signal processing techniques. Extracted features are based upon cardiac physiology and have fixed positions relative to the heartbeat. The normalization of these features makes them invariant to anxiety state. Using conventional voting techniques, the classification of heartbeats yields subject identification.

During this entire exercise, all processing was performed using robust conventional algorithms. Performance gains may be realized through an optimized classification algorithm. Optimizing the selection of a classification algorithm requires the assessment of the distribution of the extracted features over a significant population. Additional data are

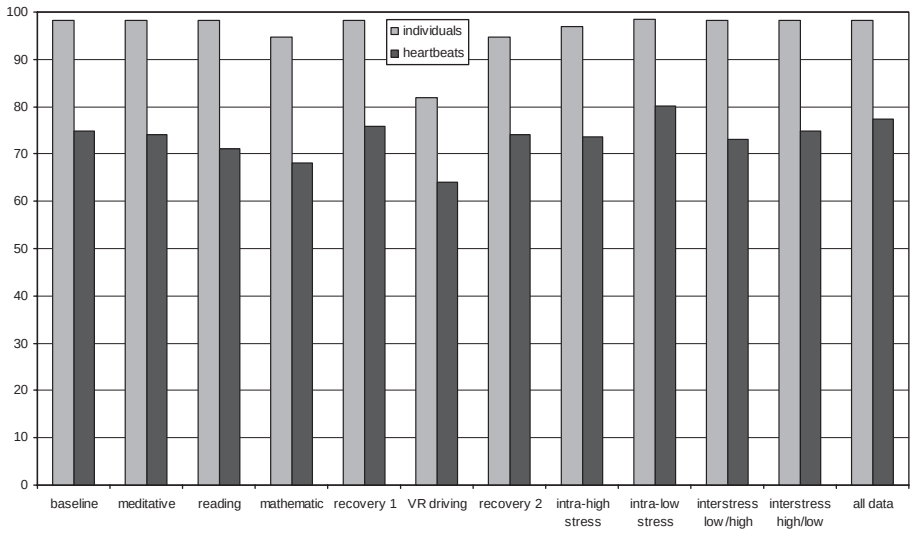

Fig. 14. Classification performance for heartbeats and identification. Labels indicate training data. Test data was the remainder of the data base. The 'all data' was an average of segments across all tasks (i.e., train segment 1–test segments 2, 3, 4, 5, and 6).

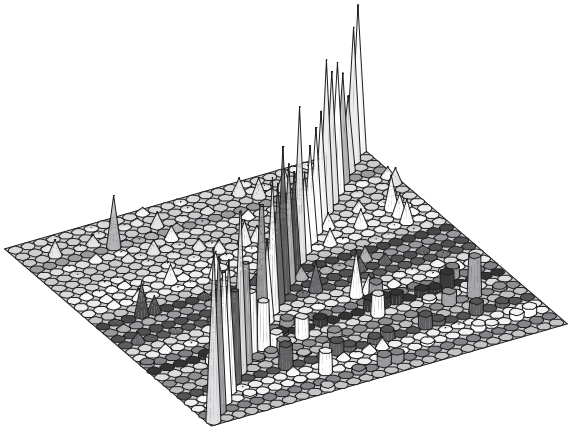

Fig. 15. Heartbeat classification for test data.

being collected to answer this and two additional questions about the ECG data: the scalability of this set of ECG features to large populations and the invariance of ECG data over significant time intervals.

7. Summary

In this paper, we show that cardiac function as expressed by the electrocardiogram (ECG) trace exhibits features that are unique to an individual. The logical series of experiments described here are quantified at each stage of processing. The experiments are divided into two categories: data processing and testing. The processing began with the characterization of noise sources in the raw data stream. From this, an optimum filter was designed to separate the cardiac information from the noise. Fiducial points were identified on the filtered data and digitally extracted. From the fiducial points, stable features were defined that characterize individuals. After the processing, the data were tested for invariance to sensor location. Next, the extracted features were tested for invariance to the individual's state of anxiety. Finally, the data set was used to identify a population of individuals. Additional data are being collected to perform two additional tests: the scalability of the features to characterize a large population, and the stability of the feature over long time intervals.

Acknowledgements

This research was sponsored by the Defense Advanced Research Projects Agency (DARPA) under contract number DABT63-00-C-1039. Additional assistance was provided by Dr. Rodney Meyer, Dr. Lauren Gavshon, Ms. Shannon McGee, and Ms. Elizabeth Rosenfeld. The authors also wish to thank Dr. P. Jonathon Phillips, DARPA, for valuable comments concerning the development of this work. The view expressed here are those of the authors and do not necessarily represent the positions of DARPA, SAIC, or VRMC.

References

[1] D. Dubin, Rapid Interpretation of ECGs, Cover, Inc., Tampa, FL, 2000.
[2] D.P. Golden Jr., R.A. Wolthuis, G.W. Hoffler, A spectral analysis of the normal resting electrocardiogram, IEEE Trans. Biomed. Eng. 20 (September 1973) 366–373.
[3] M. Malik, Heart rate variability: standards of measurement, physiological interpretation, and clinical use, Circulation 93 (5) (1996) 1043–1065.
[4] L. De Lathauwer, B. De Moor, J. Vandewalle, Fetal electrocardiogram extraction by blind source subspace separation, IEEE Trans. Biomed. Eng. 47 (5) (2000) 567–572.
[5] E. Tatara, A. Cinar, Interpreting ECG data by integrating statistical and artificial intelligence tools, IEEE Eng. Med. Biol. January/February (2002) 36–41.
[6] J. Carlson, R. Johansson, B. Olsson, Classification of electrocardiographic p-wave morphology, IEEE Trans. Biomed. Eng. 48 (4) (2001) 405–410.
[7] M. Ohlsson, H. Holst, L. Edenbrandt, Acute myocardial infarction: analysis of the ECG using artificial neural networks, in: Artificial Neural Networks in Medicine and Biology (ANNIMAB-1),Goteborg, Sweeden, 2000, pp. 209–214.
[8] L. Biel, O. Pettersson, L. Philipson, P. Wide, ECG analysis: a new approach in human identification, IEEE Trans. Instrum. Meas. 50 (3) (2001) 808–812.
[9] R. Hoekema, G.J.H. Uijen, A. van Oosterom, Geometrical aspect of the interindividual variability of multilead ECG recordings, IEEE Trans. Biomed. Eng. 48 (2001) 551–559.
[10] D.P. Jang, S.A. Israel, B.K. Wiederhold, M.D. Wiederhold, S.B. McGehee, L.W. Gavshon, R. Meyer, J.M. Irvine, Protocols for protecting patient information within a biometric analysis, in: Biometrics Section of the International Conference on Information Security, Seoul, Korea, 2001.
[11] J.M. Irvine, B.K. Wiederhold, L.W. Gavshon, S.A. Israel, S.B. McGehee, R. Meyer, M.D. Wiederhold, Heart rate variability: a new biometric for human identification, in: International Conference on Artificial Intelligence (IC-AI'2001), Las Vegas, Nevada, 2001, pp. 1106–1111.
[12] E.N. Marieb, Essential of Human Anatomy and Physiology, Benjamin Cummings Publishing Company, Inc., San Francisco, 2003.
[13] R.O. Duda, P.E. Hart, D.G. Stork, Pattern Classification, Wiley, New York, 2001.
[14] D.F. Morrison, Multivariate Statistical Methods, McGraw-Hill Inc., New York, 1976.
[15] R.G. Congalton, K. Green, Assessing the accuracy of remotely sensed data: principles and practices, Lewis Publishers, Boca Raton, FL, 1991.
[16] S.E. Fienberg, An iterative procedure for estimation in contingency tables, Ann. Math. Stat. 41 (3) (1970) 907–917.

About the Author—Dr. STEVEN A. ISRAEL is a Senior Image and Pattern Recognition Scientist at Science Applications International Corporation (SAIC). Dr. Israel analyzes non-traditional data sets for a number of government, military, and academic organizations. He received a BS (1987) and MS (1991) from the State University of New York-College of Environmental Science and Forestry. His Ph.D. (1999) was granted from the Departments of Information Science and Surveying at the University of Otago, New Zealand. Dr. Israel's interests include image processing, biometrics, photogrammetry, classification, rugby, and pattern recognition.

About the Author—Dr. JOHN M. IRVINE is the Director of Imagery Systems at Science Applications International Corporation (SAIC). He has served as chief scientist for several programs for evaluation of assisted image exploitation systems, development, and evaluation of Automatic Target Recognition (ATR) and image understanding technology, and the application of remote sensing to a range of military and civil applications. He is currently the principle investigator for the development of new, non-traditional human identification techniques (biometrics) under the DARPA HumanID Program. Dr. Irvine received his Ph.D. in 1982 in mathematical statistics from Yale University.

About the Author—Mr. ANDREW C. CHENG is a Software Engineer with SAIC. He received a BS (1997) and ME (1998) in Electrical Engineering and Computer Science from the Massachusetts Institute of Technology. His interests include aspect-oriented programming, language-neutral software platforms such as .Net, and energy alternatives such as biodiesel.

About the Author—Dr. BRENDA K. WIEDERHOLD, MBA, Ph.D., BCIA serves as Executive Director of the Virtual Reality Medical Center (VRMC), a professional medical corporation with offices in San Diego, Los Angeles, and Palo Alto, California; and as Chief Executive Officer of the Interactive Media Institute, a non-profit organization dedicated to furthering the application of advanced technologies for patient care and training. She is also a professor in the Department of Psychiatry at UCSD and a licensed clinical psychologist with national certification in both biofeedback and neurofeedback.

About the Author—Dr. MARK D. WIEDERHOLD, M.D., Ph.D., FACP serves as President of the Virtual Reality Medical Center (VRMC), a professional medical corporation with offices in San Diego, Los Angeles, and Palo Alto, California. He received a Ph.D. in 1982 from the University of Illinois Medical Center in Pathology and completed his M.D. from Rush Medical College in 1987. He completed training in internal medicine and critical care medicine at the Scripps Clinic in La Jolla. He is editor-in-chief of CyberPsychology and behavior Journal and has over 200 publications.